

Supporting Information

N-Coordinated cobalt single atoms integrated electrospun nanofibers for efficient oxygen evolution reaction

R.M. El-Shishtawy¹, M.A. Hussein^{1,2}, S.S. Al-Juaid¹, Muhammad Waseem Fazal³, Waleed

A. El-Said^{2,4*}, Naeem Akhtar^{3*}

¹*Chemistry Department, Faculty of Science, King Abdulaziz University, P.O. Box 80203, Jeddah
21589, Saudi Arabia*

²*Chemistry Department, Faculty of Science, Assiut University, Assiut, 71516 Egypt*

³*Institute of Chemical Sciences, Bahauddin Zakariya University (BZU), Multan 60800, Pakistan*

⁴*College of Science, Department of Chemistry, University of Jeddah, P.O. Box 80327, Jeddah
21589, Saudi Arabia*

Corresponding: W. A. El-Said (waahmed@uj.edu.sa), N. Akhtar (naemakhtar@bzu.edu.pk)

Section A-Instrument details

Instruments used during this scientific work were Fourier transform infrared spectroscopy (FTIR) IRA affinity-1S spectrophotometer-USA to record FTIR spectra of BM-MOF, Co-SA, cellulose acetate, polyaniline and cellulose acetate/polyaniline nanocomposite in the range of 500-4000 cm^{-1} . X-ray diffraction (XRD) was measured by Rigaku, Mini flex-II-Japan by means of Cu $K\alpha$ (with a scan angle: 5° - 80° , at 40 kV, 40 mA, and 2θ). The surface morphological analyses of the synthesized materials were analyzed using scanning electron microscopy (SEM) at a Zeiss Evo 50 XVP equipped with energy dispersive X-ray (EDAX) (Oxford instruments INCA, X.act, S.No. 56756, UK). Raman spectra was obtained using in Via Raman Microscope by RENISHAW UK with excitation laser of 514nm (laser power: 100%, grating: 1800 I/mm) and laser exposure time of 10s. Electrospinning machine (TONG LI TECH CO LTD, China) was used for the formation of nanofibers of CA/PANI composite. All the electrochemical investigations were carried out using Gamry interface (1010E) Potentio state. Th is Potentio state instrument contains three electrodes such as working electrode, reference electrode and auxiliary electrode. In this work, synthesized electrode Co-SA@SA/NF was used as working electrode, Ag/AgCl used as reference electrode and platinum wire used as auxiliary electrode.

Section B-Electrochemical experimental measurement details

A computer controlled GAMRY Potentio state workstation was used for all electrochemical studies, such as cyclic voltammetry (CV), linear sweep voltammetry (LSV), electrochemical impedance spectroscopy (EIS) and chronoamperometry into water oxidation for the test. Cyclic voltammetry was used to study redox process occurred at the electrode/electrolyte interface. The electrochemical impedance spectroscopy approach was used to measure the electrical resistance of a particular analyte.

The electrochemical experiments were performed by using standard three-electrode system which was enclosed in glass cell. In order to clean the electrochemical cell, it was washed by a mixture solution containing 3:1 of HNO_3 and H_2SO_4 and then with ultrapure distilled water. Moreover, it was rinsed numerous times first with ultrapure distilled water and then with acetone. After washing, it was dried in an oven for 30–40 minutes at 80°C . Before placing the

counter electrode, which was Pt wire, into electrochemical cell, it was washed with ultrapure water and dipped in a 20% solution of HNO₃ for a few minutes. Commercially available nickel foam (NF) treated with CN-BM-MOF and saturated silver–silver chloride (Ag|AgCl) electrode was used as working and reference electrode, respectively. At room temperature, all measurements were performed in a 1 M KOH electrolyte solution of pH of 13.5. At scan rates of 5 to 25 mV s⁻¹, CVs were determined by intentionally cycling from a positive to a negative potential. The solution of electrolyte was purified with argon gas for 30 minutes before measuring the electrochemical activity. The working electrode's geometrical area was taken into account when calculating all current values.

All potentials were recorded after 50 percent IR adjustment, which was done manually using the already reported formula:

$$E_{actual} = E_{experimental} - IR$$

The following equation was used to convert all potentials collected vs. Ag/AgCl into RHE potentials:

$$E_{RHE} = E_{Ag/AgCl} + 0.059 pH + E^0_{Ag/AgCl}$$

Here, $E_{Ag/AgCl}$ represents the measured potential against the Ag/AgCl electrode, $E^0_{Ag/AgCl}$ represents the typical thermodynamic potential (0.197 V) of Ag/AgCl, and E_{RHE} represents the estimated potential vs. RHE.

Tafel Slope calculations from the polarization curve of NC-Co-SAC@CP/NF

To evaluate the kinetics and catalytic performance, Tafel plot was plotted between over potential and log of current density in the linear portion of steady state polarization curve. It can be described using the equation.

$$\eta = a + \left(2.303 \frac{RT}{\alpha nF}\right) * \log j$$

Here, over potential is represented by η , charge transfer coefficient by α , the number of electrons take part in reaction by n , current density by j , faraday constant by F . The $2.303RT/anF$ value refers to the slope.

Section C- Results and performed calculations

Compositional Analysis of Polyaniline, Cellulose Acetate and CP

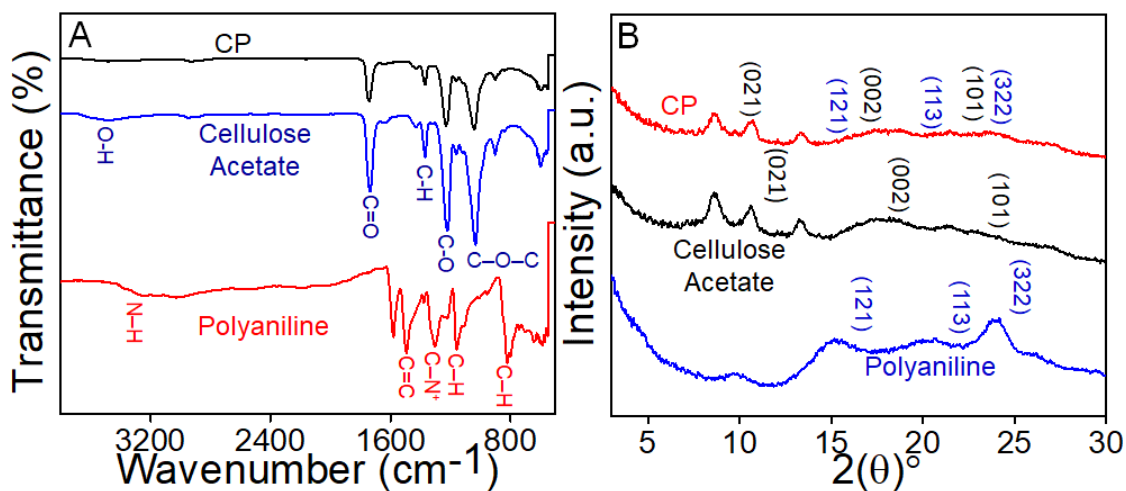


Figure S1. showing FTIR spectra of (A) Polyaniline, Cellulose Acetate and CP, whereas (B) represents XRD pattern of Polyaniline, Cellulose Acetate and CP.

Electrocatalytic activity of the NC-Co-SAC@CP/NF and BM-ZIF through LSV Analysis

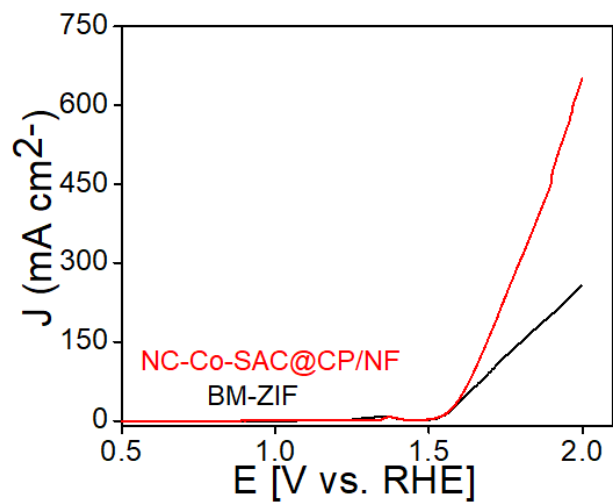


Figure S2. Electrocatalysis measurements through Linear sweep voltammetry of NC-Co-SAC@CP/NF and BM-ZIF

Electrochemically active surface area of NC-Co-SAC@CP/NF, NC-Co-SAC/NF and CP/NF

Evaluating the electrochemical double-layer capacitance and performing CV measurements at various scan ranging from 5-25 mV/s, the electrochemically active surface area of the catalyst was measured (Figure S3). By fitting the average current density vs scan rate curve, the electrochemical capacitance may be calculated easily. The CV was performed within non-faradic region. The electrochemical active area was calculated by adopting already reported method [S¹] and is given below

$$C_{dl} = slope/2$$

$$\text{Electro-active surface area} = C_{dl}/C_{sp}$$

Calculation for electrochemical active area of NC-Co-SAC@CP/NF

Straight-line equation derives from “Figure S3B” is shown in

$$J = 0.0194x - 0.185 \quad R^2 = 0.9933 \quad (S1)$$

$$C_{dl} = slope/2 = 19/2 = 9.5 \text{ mF cm}^{-2}$$

Slope = linear fit between the scan rate vs current density

$$\text{Electro-active surface area} = C_{dl}/C_{sp}$$

$$= 9.5/0.04 = 237.5 \text{ cm}^2$$

Calculation for electrochemical active area of NC-Co-SAC/NF

Straight-line equation derives from “Figure S3D” is shown in

$$J = 0.0107x + 0.029 \quad R^2 = 0.9981 \quad (S2)$$

$$C_{dl} = slope/2 = 10.7/2 = 5.35 \text{ mF cm}^{-2}$$

Slope = linear fit between the scan rate vs current density

$$\text{Electro-active surface area} = C_{dl}/C_{sp}$$

$$= 5.35/0.04 = 133.75 \text{ cm}^2$$

Calculation for electrochemical active area of CP/NF

Straight-line equation derives from “Figure S3F” is shown in

$$J = 0.0063x - 0.061 \quad R^2 = 0.8856 \quad (S3)$$

$$C_{dl} = slope/2 = 6.3/2 = 3.15 \text{ mF cm}^{-2}$$

Slope = linear fit between the scan rate vs current density

$$\text{Electro-active surface area} = C_{dl}/C_{sp}$$

$$= 3.15/0.04 = 78.75 \text{ cm}^2$$

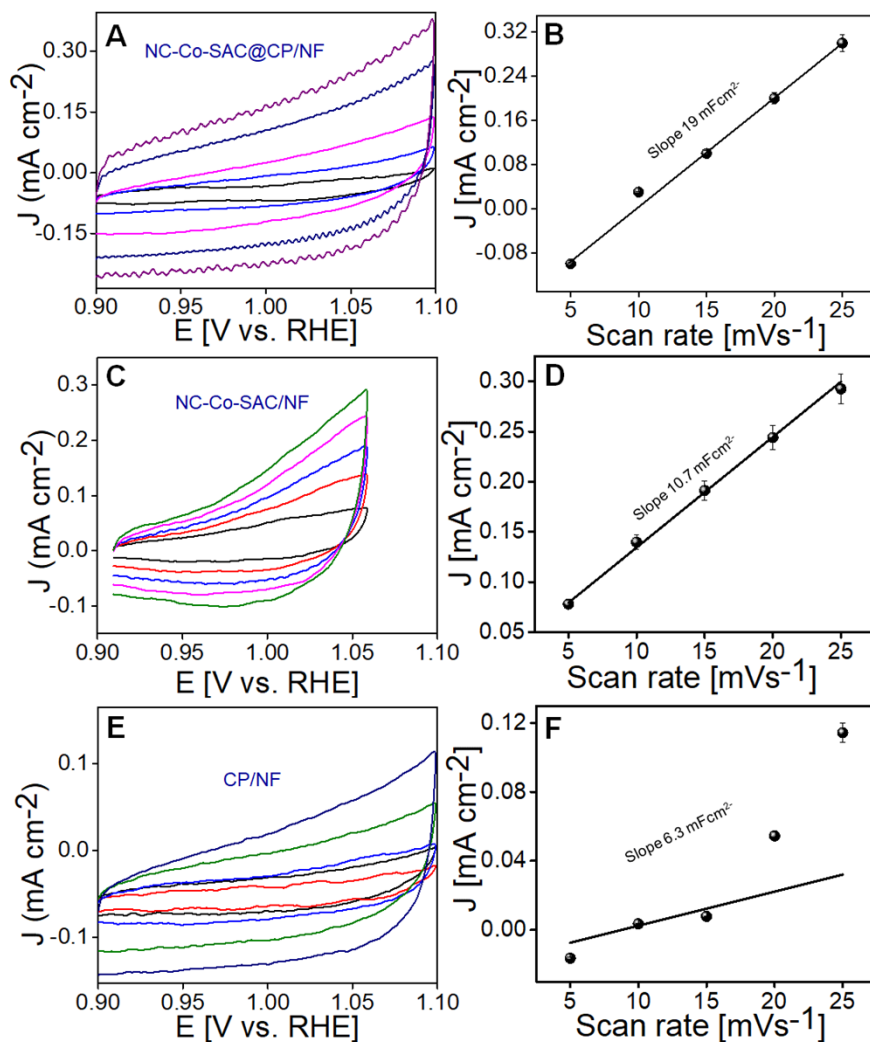


Figure S3. Evaluation of electrocatalytic activity of NC-Co-SAC@CP/NF (Figure A), NC-Co-SAC/NF (Figure C) and CP/NF (Figure E) for calculating electrochemical active area through cyclic voltammograms carried out in the non-faradaic region. Whereas, Figure B, D & E show their linear plot between scan rate and current density, respectively.

CV Analysis of CP/NF, NC-Co-SAC/NF and NC-Co-SAC@CP/NF modified electrodes

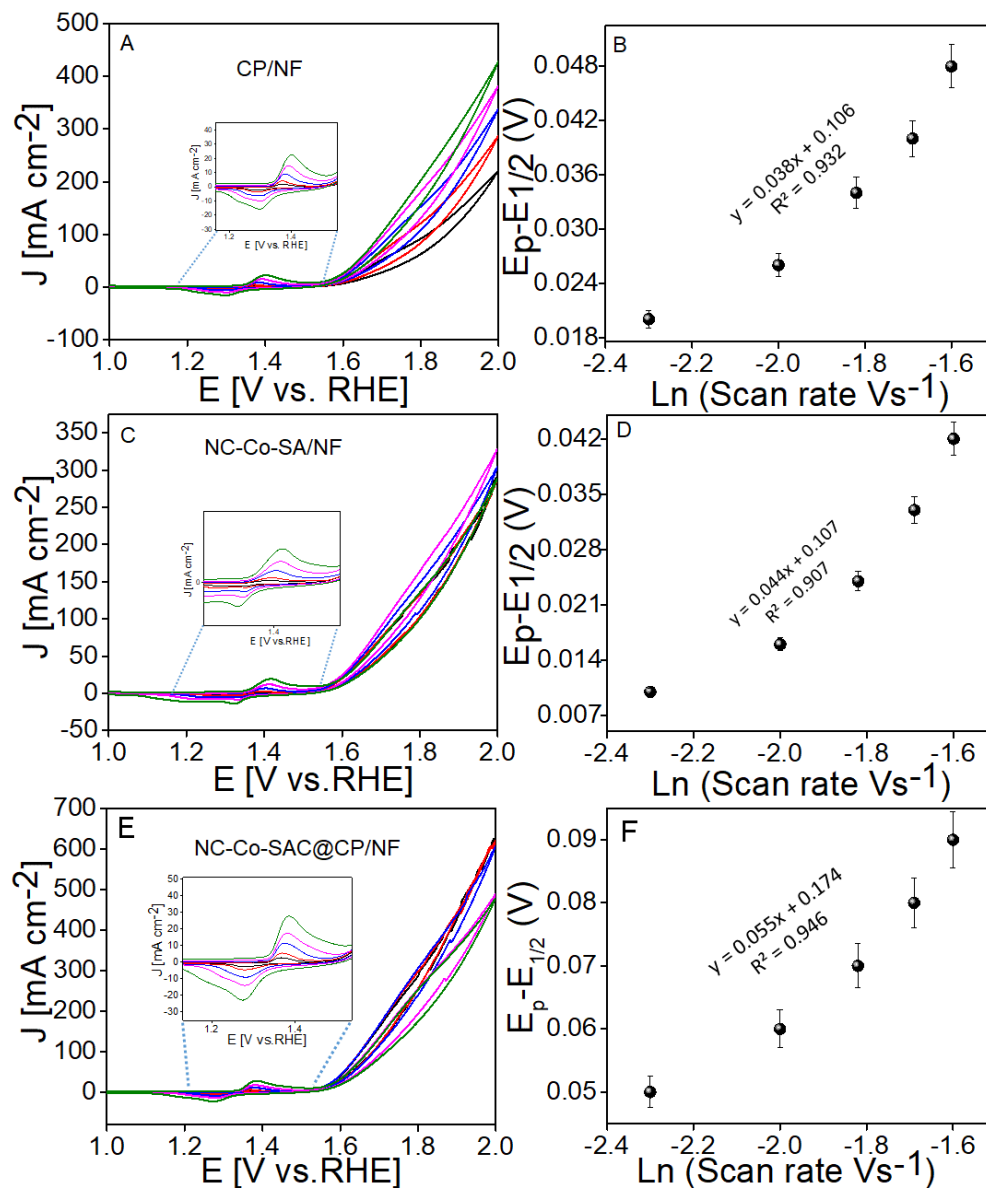


Figure S4. CV Analysis of modified electrode in Laviron equation with increasing scan rate of 5-25 mV s⁻¹ in 1 M KOH. (A) CV of CP/NF and (B) the plot of the redox peak potentials versus the logarithm of scan rates. (C) CV of NC-Co-SAC/NF and (D) the plot of the redox peak potentials versus the logarithm of scan rates (E) CV of NC-Co-SAC@CP/NF and (F) the plot of the redox peak potentials versus the logarithm of scan rates, respectively.

Stability Analysis of NC-Co-SAC@CP/NF electrode

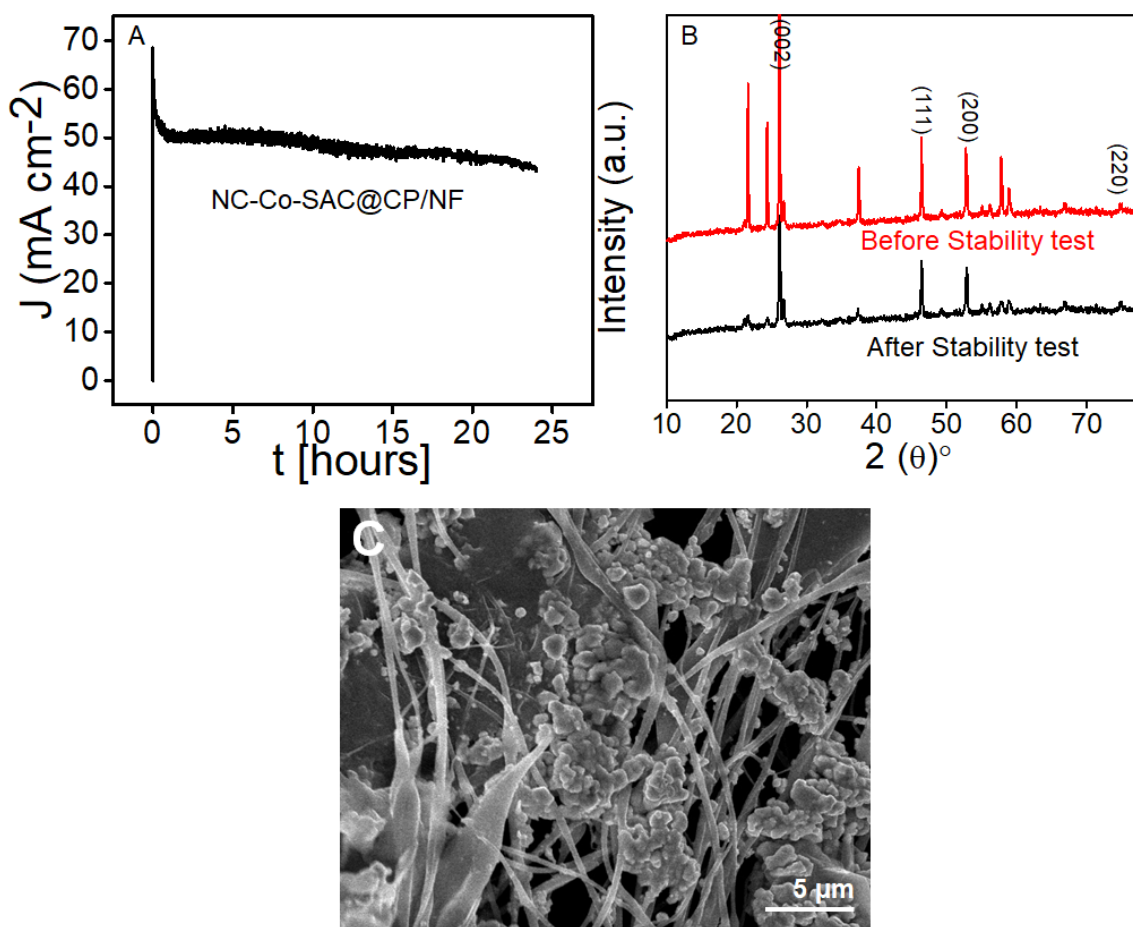


Figure S5. (A) Chronoamperometric measurement to evaluate the stability and durability for more than 24 hours at 1.60 V vs. RHE. (B) XRD spectra shows after the stability test and (C) represents the SEM image of NC-Co-SAC at the surface of CP/NF after the stability test.

Compression plot of commercial catalyst with the fabricated electrode

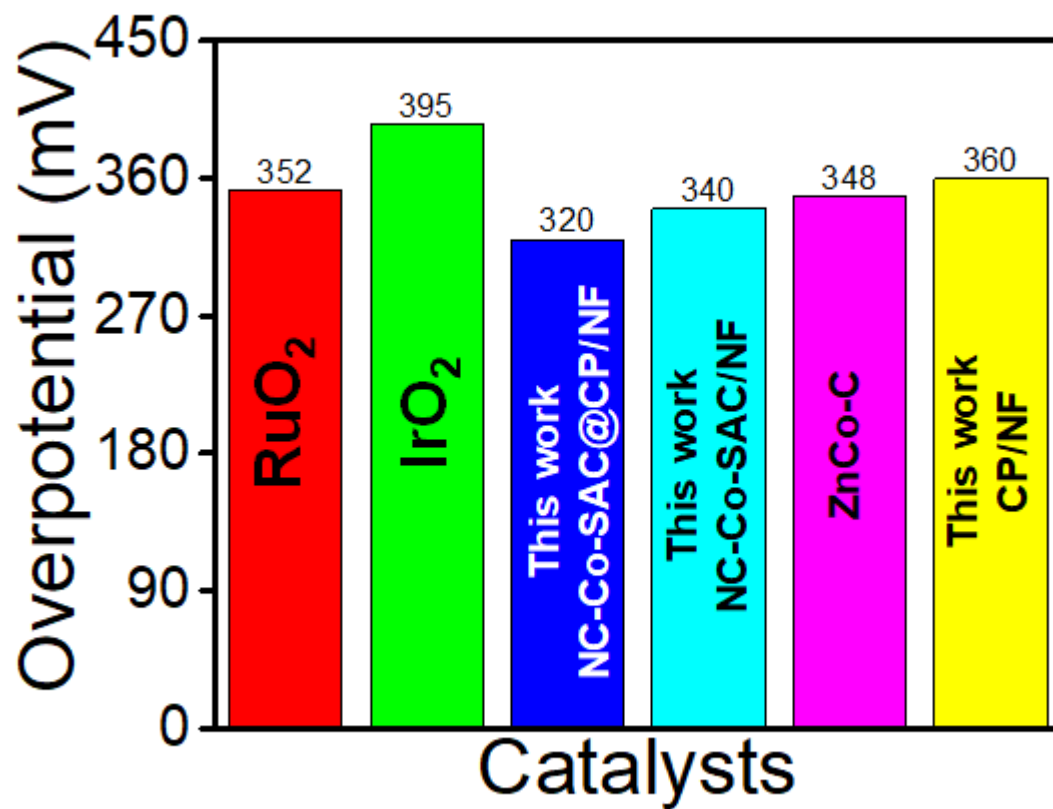


Figure S6. Compression plot (in terms over potential) of commercial catalyst with the fabricated electrode at 10 mA cm^{-2} in 1 M KOH .

Table S1. Comparison table of Tafel slope with already reported electrode

Electrode	Tafel Slope (mV/dec)	Overpotential (mV)	Electrolyte	Reference
Co ₉ S ₈ @MoS ₂ /CNFs	61	430	1.0 M KOH	S ²
NiCoP/NF	87	280	1.0 M KOH	S ³
Co ₃ O ₄ /P-CN	66.8	320	1.0 M KOH	S ⁴
Ag@ZnCo/NCF	108	279	1.0 M KOH	S ⁵
CoSAs@CNTs	85	300	1.0 M KOH	S ⁶
Co ₃ O ₄ /NiCo ₂ O ₄	88	340	1.0 M KOH	S ⁷
Co ₉ S ₈ @NOSC -900	68	330	1.0 M KOH	S ⁸
CP/NF	104	360	1.0 M KOH	This work
NC-Co-SAC/NF	72	340	1.0 M KOH	This work
NC-Co-SAC@CP/NF	59	320	1.0 M KOH	This work

Cobalt Sulfide Meets Layered Molybdenum Disulfide (Co₉S₈@MoS₂/CNFs), Cobalt Oxide Supported on Phosphorus-Doped g-C₃N₄ (Co₃O₄/P-CN), Nitrogen-doped carbon frameworks (NCF) embedded with zinc-cobalt (ZnCo) nanoparticles on the surface of Ag NWs (Ag@ZnCo/NCF), Co atoms immobilized carbon nanotubes (CoSAs@CNTs).

Reference:

1. Manzoor, S.; Abid, A. G.; Hussain, F.; Shah, A.; Pashameah, R. A.; Alzahrani, E.; El-Bahy, S. M.; Taha, T.; Ashiq, M. N. J. F., Energy conversion performance of porous ZrTe hybrid derived from chemical transformation of Zr (OH) 4. **2022**, *328*, 125264.
2. Zhu, H.; Zhang, J.; Yanzhang, R.; Du, M.; Wang, Q.; Gao, G.; Wu, J.; Wu, G.; Zhang, M.; Liu, B., When cubic cobalt sulfide meets layered molybdenum disulfide: a core-shell system toward synergetic electrocatalytic water splitting. *Advanced Materials* **2015**, *27* (32), 4752-4759.
3. Liang, H.; Gandi, A. N.; Anjum, D. H.; Wang, X.; Schwingenschlögl, U.; Alshareef, H. N., Plasma-Assisted Synthesis of NiCoP for Efficient Overall Water Splitting. *Nano Letters* **2016**, *16* (12), 7718-7725.
4. Zhu, M.; Yu, S.; Ge, R.; Feng, L.; Yu, Y.; Li, Y.; Li, W., Cobalt oxide supported on phosphorus-doped g-C₃N₄ as an efficient electrocatalyst for oxygen evolution reaction. *ACS Applied Energy Materials* **2019**, *2* (7), 4718-4729.
5. Deng, Y.; Liu, H.; Wei, X.; Ding, L.; Jiang, F.; Cao, X.; Zhou, Q.; Xiang, M.; Bai, J.; Gu, H., One-dimensional nitrogen-doped carbon frameworks embedded with zinc-cobalt nanoparticles for efficient overall water splitting. *Journal of Colloid and Interface Science* **2021**, *585*, 800-807.
6. Dilpazir, S.; He, H.; Li, Z.; Wang, M.; Lu, P.; Liu, R.; Xie, Z.; Gao, D.; Zhang, G., Cobalt Single Atoms Immobilized N-Doped Carbon Nanotubes for Enhanced Bifunctional Catalysis toward Oxygen Reduction and Oxygen Evolution Reactions. *ACS Applied Energy Materials* **2018**, *1* (7), 3283-3291.
7. Hu, H.; Guan, B.; Xia, B.; Lou, X. W. J. J. o. t. A. C. S., Designed formation of Co₃O₄/NiCo₂O₄ double-shelled nanocages with enhanced pseudocapacitive and electrocatalytic properties. **2015**, *137* (16), 5590-5595.
8. Huang, S.; Meng, Y.; He, S.; Goswami, A.; Wu, Q.; Li, J.; Tong, S.; Asefa, T.; Wu, M. J. A. f. m., N-, O-, and S-tridoped carbon-encapsulated Co₉S₈ nanomaterials: efficient bifunctional electrocatalysts for overall water splitting. **2017**, *27* (17), 1606585.